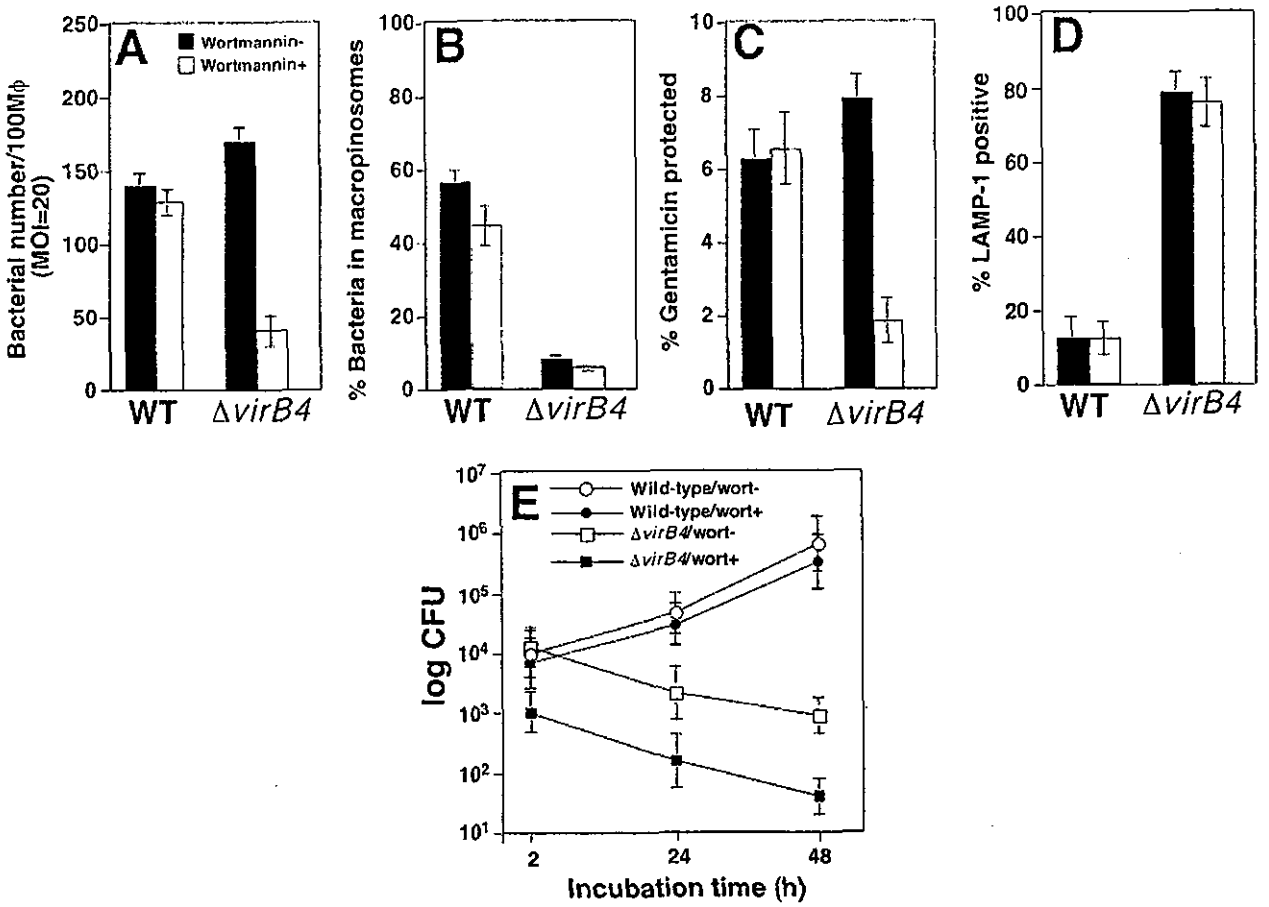

Figure 5. Effect of wortmannin treatment on *B. abortus* infection into macrophages. (A–C) Bacteria were deposited onto macrophages in the presence or absence of wortmannin and incubated at 37°C for 15 min. Uptake (A), macropinosome formation (B) or gentamicin protection (C) was quantitated as described (see Experimental procedures). Black bars: Ba600 (wild-type); open bars: Ba604 (Δ*virB4*). One hundred macrophages were examined per coverslip (A and B). Data are the average of triplicate samples from three identical experiments, and the error bars represent the standard deviation. (D) Kinetics of colocalization of LAMP-1 with phagosomes containing *B. abortus*. Ba600 (wild-type) (black bars) or Ba604 (Δ*virB4*) (open bars) was deposited onto macrophages with or without wortmannin treatment, then incubated for the periods indicated at 37°C before fixation and probing with anti-LAMP-1 antibody (see Experimental procedures). '% LAMP-1 positive' refers to percentage of internalized bacteria that showed co-staining with the LAMP-1, based on observation of 100 bacteria per coverslip. Data are the average of triplicate samples from three identical experiments, and the error bars represent the standard deviation. (E) Intracellular replication of *B. abortus* in macrophages. Macrophages in the presence or absence of wortmannin were infected with Ba600 (wild-type) or Ba604 (Δ*virB4*) as described in Experimental procedures. Data points and error bars represent the mean CFU of triplicate samples from a typical experiment (performed at least four times) and their standard deviation.

generalized plasma membrane ruffling induced by *B. abortus*.

Consistent with these observations, regulation of macropinosome formation induced by *B. abortus* was different from that induced by PMA. Inhibitor of PI3-kinase inhibits macropinocytosis, not by interfering with the initiation of the process but rather by preventing its completion [12]. PI3-kinase is necessary for macropinocytosis and phagocytosis, but not for micropinocytosis or receptor-mediated stimulation of pseudopod extension [12]. PI3-kinase contributes to a late step in the formation of macropinosomes and phagosomes, probably the closure of pseudopodia to form intracellular vesicles [12]. Our results showed that regulation of macropinosome formation induced by *B. abortus* was a mechanism independent of

PI3-kinase. Therefore, we concluded that *B. abortus* stimulates macropinosome-like novel large phagosome formation after swimming internalization.

Macropinosome formation has been described for *Legionella pneumophila*, and macropinosomes containing *L. pneumophila* included in lipid raft-associated molecules [17]. *Legionella pneumophila* modulates trafficking of phagosomes in which they reside [18]. *Legionella pneumophila* resides in phagosomes that restrict its fusion with host endosomes and lysosomes [19] and its intracellular fate is decided by the type IV transport system, Dot/Icm apparatus [20]. PI3-kinase inhibitor blocks phagocytosis of avirulent mutants, but not wild-type *L. pneumophila*, without affecting membrane ruffling and actin polymerization [21]. The mechanism of macropinosome formation by *B. abortus* and *L. pneumophila* may be similar, but swimming internalization has not been observed in *L. pneumophila* internalization and the process of initial internalization of *L. pneumophila* into mouse bone marrow-derived macrophages is still unclear.

This study showed that the early endosomal membrane-tethering molecule EEA1 was excluded in *B. abortus*-induced macropinosomes. The presence of EEA1 on phagosomes is a requisite for the subsequent acquisition of late endocytic characteristics. As EEA1 has been implicated in trafficking between the trans-Golgi network and endosomes [22] and in homotypic fusion with early endocytic compartments [23], the exclusion of this Rab5 effector from *B. abortus*-induced macropinosomes is responsible for an orderly acquisition of late endosomal membrane proteins. Consistent with this, *B. abortus*-induced macropinosomes failed to colocalize with endocytic and lysosomal marker LAMP-1. The intracellular pathway in HeLa cells of the virulent *B. abortus* strain 2308 and the attenuated strain 19 is showed [6]. Both bacterial strains are transiently detected in phagosomes characterized by the presence of early endosomal markers such as EEA1 [6]. Differences between this study and that study [6] may be caused by using different types of cell. Intracellular trafficking of *B. abortus* phagosomes is different between professional phagocytes and non-professional phagocytes [24].

EEA1 associates with oligomeric structures containing *N*-ethylmaleimide-sensitive factor (NSF) and Rabaptin-5/Rabex-5 on endosomal membranes, and interacts directly with sintaxin 13 [25]. The function of the soluble NSF attachment protein receptor (SNARE) in membrane transport is regulated by Rab proteins and their effectors [26]. Rab effectors mediate initial docking of vesicles to their target compartment, which must be synchronized with the priming of SNAREs and formation of trans-paired SNARE complexes, ultimately resulting in lipid bilayer fusion [27]. Whether SNAREs are excluded from *B. abortus*-induced macropinosomes is great interest, and needs further investigation.

Material and Methods

Reagents

Tetramethyl rhodamine isothiocyanate (TRITC)-dextran of molecular weight 155,000 (TRD × 155), phorbol myristate acetate (PMA), filipin, and wortmannin were obtained from SIGMA (St. Louis, MO, USA). Cholera toxin B subunit (CTB)-biotin conjugate was obtained from List Biological Laboratories (Campbell, CA, USA). Alexa Fluor 594-streptavidin, Cascade blue-goat anti-rabbit IgG, Texas Red-goat anti-rat IgG were obtained from Molecular Probes, Inc (Eugene, OR, USA). Rhodamine-goat anti-rabbit IgG was obtained from ICN Phamaceuticals (Aurora, OH, USA). TRITC-rabbit anti-goat IgG was obtained from Chemicon (Temecula, CA, USA). Anti-EEA1 goat polyclonal antibody was obtained from Santa Cruz Biotechnology, Inc. (Santa Cruz, CA, USA). Anti-*B. abortus* polyclonal rabbit serum was described previously [8, 28]. Anti-LAMP-1 rat monoclonal antibody 1D4B was obtained from Developmental Studies Hybridoma Bank, of the Department of Pharmacology and Molecular Sciences, Johns Hopkins University School of Medicine, Baltimore, MD, USA and the Department of Biology, University of Iowa, Iowa City, IA, USA.

Bacterial strains and media

All *B. abortus* derivatives were from 544 (ATCC23448), smooth virulent *B. abortus* biovar 1 strains. Ba598 (544 Δ*virB4*), Ba600 (544 GFP$^+$) and Ba604 (Ba598 GFP$^+$) were described previously [8, 28]. *Brucella abortus* strains were maintained as frozen glycerol stocks and were cultured on Brucella broth (Becton Dickinson and Company, Cockeysville, MD, USA) or

Brucella broth containing 1.5% agar. Kanamycin was used at 40 μg/ml.

Cell culture

Bone marrow-derived macrophages from female BALB/c mice were prepared as described [29]. After culturing in L-cell conditioned medium, the macrophages were replated for use by lifting cells in PBS on ice for 5–10 min, harvesting cells by centrifugation, and resuspending cells in RPMI 1640 containing 10% fetal bovine serum. The macrophages were seeded ($2–3 \times 10^5$ per well) in 24-well tissue culture plates for all assays.

Time lapse video microscopy

Bone marrow-derived macrophages were plated in a Lab-Tek Chambered coverglass (Nalge Nunc, Naperville, IL, USA) and were allowed to incubate overnight in RPMI 1640 containing 10% FBS at 37°C in 5% CO_2. Bacteria (2×10^6/ml) were added to the chamber, which was then placed on a heated microscope stage set to 37°C for observation by using an Olympus IX70 inverted phase microscope with 100X UPlanApo lens fitted with phase contrast optics. The bacteria were allowed to pellet passively onto the macrophages, and images were captured over a 30 min period. If further observations were desired, new samples were prepared and the procedure was initiated again.

To capture images, the lens was focused on the upper surface of the macrophage. When bacteria began to appear within the focal plane of the image, the images were captured every 15 s using a cooled charge-coupled device camera (CoolSNAP; Roper Scientific, Trenton, NJ, USA), and were processed using Openlab software (Improvision, Lexington, MA, USA) on a Power Macintosh G4 computer.

Detection of intracellular bacteria and macropinosome formation by using fluorescence microscopy

Brucella abortus strains were grown to A600 = 3.2 in Brucella broth and used to infect mouse bone marrow-derived macrophages for various periods at the indicated multiplicity of infection (MOI). Bacteria in 250 μl of RPMI 1640 containing 1 mg/ml of TRD × 155 were deposited onto the macrophages by 150 × *g* centrifugation for 5 min at room temperature, and were then incubated at 37°C, for 0 (no incubation), 5, 15, 25, and 35 min. Infected cells were fixed in periodate-lysine-paraformaldehyde (PLP) [30] containing 5% sucrose for 1 h at 37°C. The samples were washed three times in PBS, and were incubated three times for 5 min each in blocking buffer (2% goat serum in PBS) at room temperature. The samples were stained with anti-*B. abortus* polyclonal rabbit serum diluted 1:1000 in blocking buffer to identify extracellular bacteria. After incubating for 1 h at 37°C, the samples were washed three times for 5 min each with blocking buffer, were stained with Cascade blue-conjugated goat anti-rabbit IgG diluted 1:500 in blocking buffer, and were incubated for 1 h at 37°C. The samples were washed three times and were placed in mounting medium. One hundred macrophages were examined per coverslip to determine the total number of intracellular bacteria, macropinosome formation, and the total number of bacteria within macropinosome. Macropinosomes were defined as TRD × 155-labeled phagosomes in which detectable TRD × 155 surrounding the bacteria was observed by fluorescence microscopy.

Co-infection of wild-type and Δ*virB4* strain of *B. abortus*

Ba604 (Δ*virB4* GFP^+) and 544 (wild-type GFP^-) were deposited onto bone marrow-derived macrophages by 150 × *g* centrifugation at an MOI of 20 for 5 min at room temperature and were then incubated at 37°C for 15 min or 24 h. Infected macrophages were fixed in PLP-sucrose for 1 h at 37°C. The samples were washed three times in PBS, and were successively incubated three times for 5 min each in blocking buffer (2% goat serum in PBS) at room temperature. Then, the samples were permeabilized in 0.1% Triton X-100, were washed three times with blocking buffer and were incubated with anti-*B. abortus* polyclonal rabbit serum diluted 1:1000 in blocking buffer. After incubating for 1 h at 37°C, the samples were washed three times for 5 min each with blocking buffer, were stained with rhodamine-goat anti-rabbit IgG diluted 1:500 in blocking buffer, and were incubated for 1 h at 37°C. After three washes with PBS, the samples

were placed in mounting medium and visualized by fluorescence microscopy.

Measurement of the efficiency of bacterial uptake by cultured macrophages

To measure the uptake of bacteria, mouse bone marrow-derived macrophages were infected with *B. abortus* as described in the previous section. After 0, 5, 15, 25 and 35 min incubation at 37°C, macrophages were washed once with media and were incubated with 30 μg/ml gentamicin for 30 min. Macrophages were then washed three times with fresh media and were lysed with distilled water. Colony-forming units (CFU) were determined by serial dilutions on Brucella plates. Percentage protection was calculated by dividing the number of bacteria surviving the assay by the number of bacteria in the infectious inoculum, as determined by viable counts.

Measurement of the efficiency of intracellular growth of bacteria

Bacteria were deposited onto macrophages at an MOI of 20 by centrifugation at 150 × *g* for 5 min at room temperature, and were then incubated at 37°C in 5% CO_2 for 1 h. The macrophages were then washed once with medium and were incubated with 30 μg/ml gentamicin. At different time points, cells were washed and lysed with distilled water, and the number of bacteria was counted on plates of a suitable dilution.

LAMP-1 staining

Infected macrophages were fixed in PLP-sucrose for 1 h at 37°C and stained for extracellular bacteria as described above. All antibody-probing steps were for 1 h at 37°C. Samples were washed three times in PBS for 5 min and then permeabilized in −20°C methanol for 10 s. After incubating three times for 5 min with blocking buffer, samples were stained with anti-LAMP-1 rat monoclonal antibody 1D4B diluted 1:100 in blocking buffer [31]. After washing three times for 5 min in blocking buffer, samples were stained simultaneously with Texas Red-goat anti-rat IgG. Samples were placed in mounting medium and were visualized by fluorescence microscopy. Intracellular bacteria were detected by GFP fluorescence and by absence of staining with Cascade blue.

Colocalization of proteins with macropinosomes

To detect localization of GM1 ganglioside in macropinosomes, macrophage monolayers were incubated for 5 min with biotin-CTB (10 μg/ml), were rinsed three times in RPMI 1640 and were incubated with either Ba600 (wild-type) and Ba604 (Δ*virB4*) for the indicated time periods at 37°C [8]. The macrophages were washed once, were fixed in PLP-sucrose, were probed for extracellular bacteria, as above, and were permeabilized in 0.05% saponin for 10 min at room temperature. After three washes with PBS and incubation in blocking buffer, the biotin-CTB was detected by using Alexa Fluor 594-streptavidin (1:500 in blocking buffer). To detect GPI linkages, the samples fixed as above were permeabilized in methanol at −20°C for 10 s and were probed with purified aerolysin (2.5 μg/ml) for 1 h at 37°C. The antibody-probing steps of aerolysin (1:1000), and EEA1 (1:100) were the same as for LAMP-1 staining. To detect cholesterol, samples fixed as above were incubated with the fluorescent cholesterol-binding drug filipin (50 mg/ml) for 2 h at room temperature [8].

Drug treatment

PMA and wortmannin treatments were done by the method of Araki *et al.* [12]. Briefly, mouse bone marrow-derived macrophages were incubated with RPMI 1640 containing 30 ng/ml PMA or 100 nM wortmannin for 30 min at 37°C. After washing with media containing PMA or wortmaninn, the macrophages were infected with bacteria as described in the previous section.

Acknowledgements

This work was supported, in part, by grants from Grant-in-Aid for Scientific Research (12575029 and 13770129), Japan Society for the Promotion of Science, and by the Sasakawa Scientific Research Grant from The Japan Science Society.

References

1 Lopes MF, Freire-de-Lima CG, DosReis GA. The macrophage haunted by cell ghosts: a pathogen grows. *Immunol Today* 2000; **21**: 489–94.
2 Dorn BR, Dunn WA Jr, Progulske-Fox A. Bacterial interactions with the autophagic pathway. *Cell Microbiol* 2002; **4**: 1–10.
3 Méresse S, Steele-Mortimer O, Moreno E, Desjardins M, Finlay B, Gorvel J. Controlling the maturation of pathogen-containing vacuoles: a matter of life and death. *Nat Cell Biol* 1919; **1**: 183–8.
4 Baldwin CL, Winter AJ. Macrophages and *Brucella*. *Immunol Ser* 1994; **60**: 363–80.
5 Comerci DJ, Martinez-Lorenzo MJ, Sieira R, Gorvel J, Ugalde RA. Essential role of the VirB machinery in the maturation of the *Brucella abortus*-containing vacuole. *Cell Microbiol* 2001; **3**: 159–68.
6 Pizarro-Cerda J, Méresse S, Parton RG *et al*. *Brucella abortus* transits through the autophagic pathway and replicates in the endoplasmic reticulum of nonprofessional phagocytes. *Infect Immun* 1998; **66**: 5711–24.
7 Pizarro-Cerda J, Moreno E, Sanguedolce V, Mege JL, Gorvel JP. Virulent *Brucella abortus* prevents lysosome fusion and is distributed within autophagosome-like compartments. *Infect Immun* 1998; **66**: 2387–92.
8 Watarai M, Makino S-I, Fujii Y, Okamoto K, Shirahata T. Modulation of *Brucella*-induced macropinocytosis by lipid rafts mediates intracellular replication. *Cell Microbiol* 2002; **4**: 341–56.
9 Racoosin EL, Swanson JA Macrophage colony-stimulating factor (rM-CSF) stimulates pinocytosis in bone marrow-derived macrophages. *J Exp Med* 1989; **170**, 1635-48.
10 Swanson JA. Phorbol esters stimulate macropinocytosis and solute flow through macrophages. *J Cell Sci* 1989; **94**: 135–42.
11 Watarai M, Makino S-I, Michikawa M, Yanagisawa K, Murakami S, Shirahata T. Macrophage plasma membrane cholesterol contributes to *Brucella abortus* infection mice. *Infect Immun* 2002; **70**: 4818–25.
12 Araki N, Johnson MT, Swanson JA. A role for phosphoinositide 3-kinase in the completion of macropinocytosis and phagocytosis by macrophages. *J Cell Biol* 1996; **135**: 1249–60.
13 Arcaro A, Wymann MP. Wortmannin is a potent phosphatidylinositol 3-kinase inhibitor: the role of phosphatidylinositol 3,4,5-trisphosphate in neutrophil responses. *Biochem J* 1993; **296**: 297–301.
14 Racoosin EL, Swanson JA. M-CSF-induced macropinocytosis increases solute endocytosis but not receptor-mediated endocytosis in mouse macrophages. *J Cell Sci* 1992; **102**: 867–80.
15 Watts C, Marsh M. Endocytosis: what goes in and how? *J Cell Sci* 1992; **103**: 1–8.
16 Swanson JA, Watts C. Macropinocytosis. *Trend Cell Biol* 1995; **5**: 424–8.
17 Watarai M, Derre I, Kirby J, Growney JD, Dietrich WF, Isberg RR. *Legionella pneumophila* is internalized by a macropinocytotic uptake pathway controlled by the Dot/Icm system and the mouse *Lgn1* locus. *J Exp Med* 2001; **194**: 1081–95.
18 Vogel JP, Isberg RR. Cell Biology of *Legionella pneumophila*. *Curr Opinions Microbiol* 1999; **2**: 30–4.
19 Horwitz MA. The Legionnaires' disease bacterium (*Legionella pneumophila*) inhibits phagosome-lysosome fusion in human monocytes. *J Exp Med* 1983; **158**: 1319–31.
20 Christie PJ, Vogel JP. Bacterial type IV secretion: conjugation systems adapted to deliver effector molecules to host cells. *Trend Microbiol* 2000; **8**: 354–60.
21 Khelef N, Shuman HA, Maxfield FR. Phagocytosis of wild-type *Legionella pneumophila* occurs through a wortmannin-insensitive pathway. *Infect Immun* 2001; **69**: 5157–16.
22 Simonsen A, Gaullier JM, D'Arrigo A, Stenmark H. The Rab5 effector EEA1 interacts directly with syntaxin-6. *J Biol Chem* 1999; **274**: 28857–60.
23 Simonsen A, Lippe R, Christoforidis S *et al*. EEA1 links PI(3)K function to Rab5 regulation of endosome fusion. *Nature* 1998; **394**: 494–8.
24 Arenas GN, Staskevich AS, Aballay A, Mayorga LS. Intracellular trafficking of *Brucella abortus* in J774 macrophages. *Infect Immun* 2000; **68**: 4255–63.
25 McBride HM, Rybin V, Murphy C, Giner A, Teasdale R, Zerial M. Oligomeric complexes link Rab5 effectors with NSF and drive membrane fusion via interactions between *EEA1* and syntaxin 13. *Cell* 1999; **98**: 377–86.
26 Novick P, Zerial M. The diversity of Rab proteins in vesicle transport. *Curr Opin Cell Biol* 1990; **9**: 496–504.
27 Weber T, Zemelman BV, McNew JA *et al*. SNAREpins: minimal machinery for membrane fusion. *Cell* 1998; **92**: 759–72.
28 Watarai M, Makino S-I, Shirahata T. An essential virulence protein of *Brucella abortus*, VirB4, requires an intact nucleoside triphosphate-binding domain. *Microbiology* 2002; **148**: 1439–46.
29 Watarai M, Andrews HL, Isberg RR. Formation of a fibrous structure on the surface of *Legionella pneumophila* associated with exposure of DotH and DotO proteins after intracellular growth. *Mol Microbiol* 2001: **39**: 313–29.
30 McLean IW, Nakane PK. Periodate-lysine-paraformaldehyde fixative: a new fixative for immunoelectron microscopy. *J Histochem Cytochem* 1974; **22**: 1077–83.
31 Swanson MS, Isberg RR. Identification of *Legionella pneumophila* mutants that have aberrant intracellular fates. *Infect Immun* 1996; **64**: 2585–94.

Case Report

Respiration

Respiration 2002;69:547–549
DOI: 10.1159/000066463

Received: August 6, 2001
Accepted after revision: February 12, 2002

Mycobacterium avium Complex Pleuritis

Katsunori Yanagihara Kazunori Tomono Toyomitsu Sawai
Yoshitsugu Miyazaki Yoichi Hirakata Jun-Ichi Kadota Shigeru Kohno

The Second Department of Internal Medicine, Nagasaki University School of Medicine, Nagasaki, Japan

Key Words
Mycobacterium avium complex · Pleuritis · Non-immunocompromised

Abstract
Non-tuberculous mycobacterium infection is rarely accompanied by pleural involvement. We report a very rare case of *Mycobacterium avium-intracellurare* complex (MAC) pleuritis with massive pleural effusion. The patient was a non-compromised 67-year-old female and had been treated for pulmonary non-tuberculous mycobacterium infection. She was admitted to hospital because of general malaise, low-grade fever and right pleural effusion. Cytological examination of the effusion did not show malignant cells. MAC was only identified by culture and PCR. No other bacteria were detected. Complete resolution of the pleural effusion occurred after administration of anti-tubercular agents (isoniazid, rifampin, ethambutol) and clarithromycin.

Introduction

Moist pleurisy in patients with *Mycobacterium avium* complex (MAC) is rarer than tuberculosis. It has been reported that MAC-related disease begins with centriacinar abnormalities in the lung, and the incidence of lymphatic abnormality is low. Tuberculosis (idiopathic pleuritic type) is thought to cause pleuritis associated with pleural effusion from the primary focus of a pulmonary infection. Thus the onset of unilateral effusion is extremely rare in patients with MAC disease.

We report a rare case of a non-immunocompromised Japanese woman with MAC pleuritis.

Case Report

The patient was a 67-year-old Japanese woman. She was admitted to Nagasaki University Hospital because of general malaise, low-grade fever and right pleural effusion. Physical examination showed the patient was 155 cm tall, weighed 60 kg and had an arterial blood pressure of 126/76 mm Hg, a pulse rate of 96/min and a temperature of 37.3°C. Coarse crackles were present over the right lower lung field. There was no lymphadenopathy.

Laboratory tests showed the erythrocyte sedimentation rate to be 72 mm/h, leucocyte count 4.5 × 10^9/l. Total proteins were 6.9 g/dl, with low albumin (54.8%). A human immunodeficiency virus (HIV) antibody test was negative. Tuberculin skin test reading was 15 mm.

KARGER
Fax + 41 61 306 12 34
E-Mail karger@karger.ch
www.karger.com

0025–7931/02/0696–0547$18.50/0

Accessible online at:
www.karger.com/res

Katsunori Yanagihara, MD, PhD
The Second Department of Internal Medicine
Nagasaki University School of Medicine
1-7-1 Sakamoto, Nagasaki, 852 (Japan)
Tel. +81 95 849 7276, Fax +81 95 849 7285, E-Mail kyana-ngs@umin.ac.jp

Fig. 1. Posteroanterior chest roentgenogram at the time of admission. Note the presence of the pleural effusion in the left thorax.

Fig. 2. Posteroanterior chest roentgenogram taken at the time of discharge. Note the complete resolution of the pleural effusion.

Chest X-ray (fig. 1) and computed tomography showed a massive pleural effusion in the right lower region and pulmonary opacities in the right middle and lower lung fields, as well as in the left lower lung field. Bacteriological examination and culture of sputum showed the presence of MAC. No other bacteria were detected. The pleural fluid was yellowish clear with a specific gravity of 1.035. Cytological examination of the effusion did not show any malignant cells. Biochemical analysis of the effusion showed a protein level of 5.2 g/dl (serum protein 6.9 g/dl), lactose dehydrogenase 1,125 U/l, and Rivalta reaction was positive. Bacteriological examinations, staining and culture of the fluid were negative. MAC was identified in the pleural effusion by culture and PCR using Amplicor Mycobacterium.

Based on the clinical findings and laboratory data, our diagnosis was pulmonary disease and pleuritis due to MAC.

The treatment started with isoniazid 400 mg/day, rifampin 450 mg/day, ethambutol hydrochloride 500 mg/day and clarithromycin 800 mg/day. A gradual improvement in the clinical features was observed with ongoing treatment. The patient was discharged free of symptoms three months after admission. A chest roentgenogram taken at the time of discharge showed a complete resolution of the pleural effusion (fig. 2). She continued the same treatment for another three months and was seen regularly at the outpatient clinic. A close follow-up for more than two years after her discharge from the hospital indicates that the clinical course has remained unremarkable.

Discussion

It is generally assumed that when non-tuberculous mycobacterium is isolated from a closed space, it is responsible for the pathological changes observed. However, non-tuberculous mycobacteria can be isolated from the pleural effusion in untreated patients with non-tuberculous mycobacterium infections, such as those with congestive heart failure and metastatic tumours [1]. In the present case, the patient did not have such an underlying disease. The clinical features of this case were typical for pleuritis. As we could only detect MAC in the pleural space and the sputum, we diagnosed the condition as MAC pleuritis.

Our patient was confirmed to be free of any coexisting immunodeficiency, such as AIDS. Pleural involvement without HIV infection has been reported in a patient with disseminated MAC infection. However, primary MAC pleuritis without MAC infection is extremely rare. Okada et al. [2] reported MAC pleuritis in a non-immunocompromised 35-year-old male. They indicated that the unusually massive retention of pleural effusion was due to a lack of treatment for approximately three months following the onset of the pleuritis [2]. Although our case was carefully followed in the outpatient department, the pleural effusion increased rapidly in volume. Previous studies have indicated that malnutrition, impaired cellular immunity, apparently abnormal microvascular circulation due to diabetes mellitus [3] and surgical treatment [4] may enhance the development of pleuritis in infections caused by MAC. Our patient showed no clinical features or laboratory test results indicative of a dysfunctional immune system. However, she could have underlying fibro-bullous changes as a possible explanation for the development of MAC disease.

Recently, Takahashi et al. [5] suggested that MAC may be linked to a disease susceptibility gene and be determined by human leucocyte-associated antigens in patients with pulmonary MAC infections. Their results suggest that some Japanese individuals may be susceptible to MAC infections.

Although the exact reason for the onset of pleuritis is yet unknown, our case suggests pleuritis should be considered in patients with pulmonary infections caused by nontuberculous mycobacteria. Physicians should be aware of MAC pleuritis even in non-immunocompromised patients.

References

1 Gribetz AR, Damsker B, Marchevsky A, et al: Nontuberculosis mycobacteria in pleural fluid. Chest 1985;87:495–498.

2 Okada Y, Ichinose Y, Yamaguchi K, et al: *Mycobacterium avium-intracellulare* pleuritis with massive pleural effusion. Eur Respir J 1995;8:1428–1429.

3 Nagaia T, Akiyama M, Yoshinori M, et al: *Mycobacterium avium* complex pleuritis accompanied by diabetes mellitus. Diabetes Res Clin Pract 2000;48:99–104.

4 Kawamoto H, Yamagata M, Nakashima H, et al: Development of a case of *Mycobacterium avium* complex disease from right pleural effusion. Nihon Kokyuki Gakkai Zasshi 2000;38: 706–709.

5 Takahashi M, Ishizuka A, Nakamura H, et al: Specific HLA in pulmonary MAC infection in a Japanese population. Am J Respir Crit Care Med 2000;162:316–318.

Microbiol. Immunol., 47(2), 161–165, 2003

Screening Method for *Salmonella enterica* Serovar Typhi and Serovar Paratyphi A with Reduced Susceptibility to Fluoroquinolones by PCR-Restriction Fragment Length Polymorphism

Kenji Hirose, Kazumichi Tamura, and Haruo Watanabe*

Department of Bacteriology, National Institute of Infectious Diseases, Shinjuku-ku, Tokyo 162–8640, Japan

Received October 15, 2002; in revised form, November 21, 2002. Accepted November 25, 2002

***Abstract*: *Salmonella enterica* serovar Typhi and serovar Paratyphi A with reduced susceptibility to fluoroquinolones (MICs of ciprofloxacin, 0.25 to 2 μg/ml) have a mutation at codon either Ser-83 or Asp-87 of *gyrA* gene. A screening method by PCR-restriction fragment length polymorphism (PCR-RFLP) was designed to screen the mutations at codon Ser-83 and Asp-87 of the *gyrA* gene of *S. enterica* serovar Typhi and serovar Paratyphi A clinical isolates. This method successfully screened the *gyrA* mutations of *S. enterica* serovar Typhi and serovar Paratyphi A with reduced susceptibility to fluoroquinolones.**

***Key words*: *Salmonella enterica* serovar Typhi, *Salmonella enterica* serovar Paratyphi A, RFLP, Fluoroquinolone resistance**

Typhoid fever is sometimes a fatal infection to adults and children that causes bacteremia and inflammatory destruction of the intestine and other organs and requires the urgent treatment by the administration of appropriate antibiotics. Recently, fluoroquinolone has proven to be effective for the treatment of typhoid fever, which becomes the first-line drug for the treatment of typhoid fever (3, 10, 13, 17). However, *S. enterica* serovar Typhi strains resistant to fluoroquinolones and with reduced susceptibility to fluoroquinolones have been already reported (2, 6, 11, 14–16). Further, several clinical treatment failures with ciprofloxacin and other fluoroquinolones to typhoid patients infected by the strains with reduced susceptibility to fluoroquinolones have also been reported (12, 16). The emergence and spread of the strains with reduced susceptibility to fluoroquinolones have been reported in several developing countries and also in Japan. The mechanisms of fluoroquinolone resistance have been well studied. Most of the acquired resistant phenotype were attributed to mutations in the genes encoding DNA gyrase (*gyrA*, *gyrB*) or DNA topoisomerase IV (*parC*, *parE*) (7–9, 18–20). The alterations at the codon Ser-83 and Asp-87 of GyrA are the most frequently found in the clinical isolates with reduced susceptibility to fluoroquinolones in *S. enterica* serovar Typhi and serovar Paratyphi A (1, 5). We previously reported that only *gyrA* mutations contribute to the fluoroquinolone resistance in *S. enterica* serovar Typhi and serovar Paratyphi A. Any *gyrB*, *parC* and *parE* mutations which are responsible for the fluoroquinolone resistance were not found in the clinical isolates of *S. enterica* serovar Typhi and serovar Paratyphi A in our previous study (5). The susceptibility test by diffusion with nalidixic acid disk is now employed for the screen of the strains with reduced susceptibility to fluoroquinolones. However, alternate DNA based method is required for the rapid screening for the strains with reduced susceptibility to fluoroquinolones. The purpose of this study is to develop more rapid screening method for the detection of fluoroquinolone resistant strains and the strain with reduced susceptibility to fluoroquinolones than the ordinary culture method.

The bacterial strains used in this study were collected from the regional public health offices in Japan and all isolates were obtained from either a blood culture or a stool culture of individual patients and identified by

**Address correspondence to* Dr. Haruo Watanabe, Department of Bacteriology, National Institute of Infectious Diseases, 1–23–1, Toyama, Shinjuku-ku, Tokyo 162–8640, Japan. Fax: +81–3–5285–1171. E-mail: haruwata@nih.go.jp

Abbreviations: Asp, aspartic acid; MIC, minimum inhibitory concentration; PCR, polymerase chain reaction; QRDR, quinolone resistance determining region; RFLP, restriction fragment length polymorphism; Ser, serine.

Table 1. Primers used for PCR-RFLP

Primers	Sequence	Primer position[a]
gyrA-F	5'-TGT CCG AGA TGG CCT GAA GC -3'	108–127
gyrA-HinfI-as	5'-ATG TAA CGC AGC GAG AAT GGC TGC GCC ATA CGA ACG CTG GA*[b]G -3'	302–261

[a] The primer positions were indicated by the number of nucleotide sequences from the start codon of *gyrA* gene.
[b] The mismatch sequence to produce a *Hinf*I site into the amplified fragment is indicated by asterisc on the primer of gyrA-HinfI-as.

biochemical tests and serological tests on the basis of standard criteria. The ciprofloxacin resistant strains were selected by culturing the ciprofloxacin susceptible strains or the strains with decreased susceptibility to ciprofloxacin in the medium supplemented with ciprofloxacin (4). A total of 32 strains of *S. enterica* serovar Typhi (3 ciprofloxacin resistant strains, 25 clinical isolates with reduced susceptibility to ciprofloxacin and 4 ciprofloxacin susceptible strains) and 15 strains of *S. enterica* serovar Paratyphi A (4 ciprofloxacin resistant strains, 7 clinical isolates with reduced susceptibility to ciprofloxacin and 4 ciprofloxacin susceptible strains) were used for this study (5). The MICs of ciprofloxacin and nalidixic acid were determined by Etest (AB Biodisk, Solna, Sweden), according to the manufacturer's instructions. The determination of *gyrA* mutations were previously described (4, 5). The PCR-RFLP method of screening *gyrA* mutations for *Salmonella typhimurium* was previously described by Giraud et al., which was used in this study with a slight modification for *S. enterica* serovar Typhi and serovar Paratyphi A (4). We designed the PCR-RFLP to detect common mutations related to fluoroquinolone resistance at codon Ser-83 and Asp-87 of GyrA. The PCR was performed with the primers, gyrA-F and gyrA-HinfI-as, which is expected to produce a 195-bp amplified fragment with two *Hinf*I restriction sites at the codon corresponding to Ser-83 and Asp-87 of GyrA; the reverse primer gyrA-HinfI-as, whose sequence is different by one base from the original gene sequence, introduced an artificial *Hinf*I cleavage site at Asp-87 codon of GyrA according to the primer-specified restriction site modification method (Table 1). Restriction enzyme digestions were performed in a total of 20 μl of the mixture containing 10 μl of PCR product, 2 μl of 10× digestion buffer and 5 U of *Hinf*I for 60 min incubation at 37 C. The digested PCR products were separated in 15% polyacrylamide gel electrophoresis.

The alterations of the *gyrA* gene have a major role in the fluoroquinolone resistance of gram negative bacteria among the mechanisms of quinolone resistance. Our data in previous study showed that only the strains with reduced susceptibility to fluoroquinolones were found in the clinical isolates, and that the typical resistant strains (MIC of ciprofloxacin; ≥4 μg/ml) were never found. We determined the *gyrA* mutations of more than 100 strains of *S. enterica* serovar Typhi and serovar Paratyphi A with reduced susceptibility to fluoroquinolones. *S. enterica* serovar Typhi and serovar Paratyphi A clinical isolates with reduced susceptibility to fluoroquinolones had only a single mutation in the *gyrA* gene at the position of either Ser-83 or Asp-87 of GyrA (Table 2), and other *gyrA* mutations were never found in the clinical isolates of *S. enterica* serovar Typhi and serovar Paratyphi A. The alterations in the quinolone resistance determining regions (QRDR) of the *gyrB* and *parE* genes were not found in all of the clinical strains tested. The typical fluoroquinolone resistant strains (MIC of ciprofloxacin; ≧4 μg/ml), which were obtained by experimental selection *in vitro*, had mutations at both of Ser-83 and Asp-87 of GyrA (Table 2). Our previous findings clearly showed that *gyrA* mutations were essentially involved in the reduced susceptibility to fluoroquinolones and fluoroquinolone resistance of *S. enterica* serovar Typhi and serovar Paratyphi A. Therefore, the screening of *gyrA* mutations is considered to be necessary and sufficient for the screening of the strains with reduced susceptibility to fluoroquinolones in *S. enterica* serovar Typhi and serovar Paratyphi A.

A fragment including *gyrA* QRDR was amplified by PCR with the primers gyrA-F and gyrA-HinfI-as (Table 1). The size of the amplified fragment was 195 bp, which is the same in all *S. enterica* serovar Typhi and serovar Paratyphi A strains tested. After *Hinf*I digestion, the cleaved fragments of the susceptible strains of *S. enterica* serovar Typhi and serovar Paratyphi A consisted of 3 bands (137, 43 and 15 bp; RFLP pattern D in Fig. 1), which was produced by the *Hinf*I sites at the nucleotide sequences corresponding to Ser-83 and Asp-87 of GyrA. The 15-bp smallest fragment, which was produced by the cleavage between Ser-83 and Asp-87 of GyrA, was invisible in Fig. 1, however, it is easy to be differentiated from the other types. The digested fragment of the strains which have a mutation in codon Ser-83 of GyrA consist of 2 bands (152 and 43 bp; RFLP pattern B in Fig. 1), which lost the *Hinf*I site corresponding to the Ser-83 of GyrA. The fragment of the strains which have a mutation in codon Asp-87 of GyrA consist of 2 bands (137 and 58 bp; RFLP pattern C in Fig. 1). The fragment of the strains which have mutations in both Ser-83 and Asp-87 were not digested by

Table 2. The results of RFLP patterns, MICs and *gyrA* muations of each strains

Serovar	Strain No.	MIC (μg/ml)		*gyrA*[c]		RFLP-pattern [d]
		CPFX[a]	NA[a]	83 TCC (Ser)	87 GAC (Asp)	
Typhi	NIHP3-4[b]	>32	>256	TTC (Phe)	TAC (Tyr)	A
Paratyphi A	NIHP3-1[b]	>32	>256	TTC (Phe)	AAC (Asn)	A
Typhi	NIHP3-43[b]	16	>256	TTC (Phe)	TAC (Tyr)	A
Typhi	NIHP3-39[b]	8	>256	TTC (Phe)	TAC (Tyr)	A
Paratyphi A	NIHP3-44[b]	8	>256	TTC (Phe)	TAC (Tyr)	A
Paratyphi A	NIHP3-3[b]	8	>256	TTC (Phe)	TAC (Tyr)	A
Paratyphi A	NIHP3-41[b]	8	>256	TTC (Phe)	TAC (Tyr)	A
Paratyphi A	950040	2	>256	TTC (Phe)	None	B
Typhi	000006	0.5	>256	TAC (Tyr)	None	B
Typhi	000007	0.5	>256	TAC (Tyr)	None	B
Typhi	000008	0.5	>256	TAC (Tyr)	None	B
Typhi	000009	0.5	>256	TAC (Tyr)	None	B
Typhi	000012	0.5	>256	TAC (Tyr)	None	B
Typhi	000015	0.5	>256	None	GGC (Gly)	C
Typhi	000016	0.5	>256	TAC (Tyr)	None	B
Typhi	000019	0.5	>256	TAC (Tyr)	None	B
Typhi	990069	0.5	>256	TAC (Tyr)	None	B
Typhi	990026	0.5	>256	TAC (Tyr)	None	B
Typhi	980083	0.5	>256	TAC (Tyr)	None	B
Typhi	990106	0.5	>256	TTC (Phe)	None	B
Typhi	990097	0.5	>256	TAC (Tyr)	None	B
Typhi	000022	0.5	>256	TAC (Tyr)	None	B
Typhi	000023	0.5	>256	TAC (Tyr)	None	B
Typhi	000025	0.5	>256	TAC (Tyr)	None	B
Paratyphi A	990112	0.5	>256	TTC (Phe)	None	B
Paratyphi A	990110	0.5	>256	TTC (Phe)	None	B
Paratyphi A	000040	0.5	>256	TTC (Phe)	None	B
Paratyphi A	000055	0.5	>256	TTC (Phe)	None	B
Paratyphi A	990021	0.5	>256	TTC (Phe)	None	B
Paratyphi A	980043	0.5	>256	TTC (Phe)	None	B
Typhi	990018	0.25	>256	TTC (Phe)	None	B
Typhi	990120	0.25	>256	TTC (Phe)	None	B
Typhi	990102	0.25	>256	TTC (Phe)	None	B
Typhi	970004	0.25	>256	TTC (Phe)	None	B
Typhi	990020	0.25	>256	None	GGC (Gly)	C
Typhi	990104	0.25	64	TTC (Phe)	None	B
Typhi	000015	0.25	64	None	TAC (Tyr)	C
Typhi	000027	0.25	64	None	TAC (Tyr)	C
Typhi	000037	0.25	64	None	TAC (Tyr)	C
Paratyphi A	970131	0.032	4	None	None	D
Paratyphi A	000066	0.016	4	None	None	D
Paratyphi A	990118	0.064	2	None	None	D
Typhi	990100	0.032	2	None	None	D
Typhi	990113	0.016	2	None	None	D
Typhi	010053	0.016	2	None	None	D
Typhi	010063	0.016	2	None	None	D
Paratyphi A	010044	0.032	1	None	None	D

[a] CPFX, ciprofloxacin; NA, nalidixic acid.
[b] Mutants experimentally selected *in vitro*.
[c] None, no mutations were found.
[d] The digested patterns in Fig. 1.

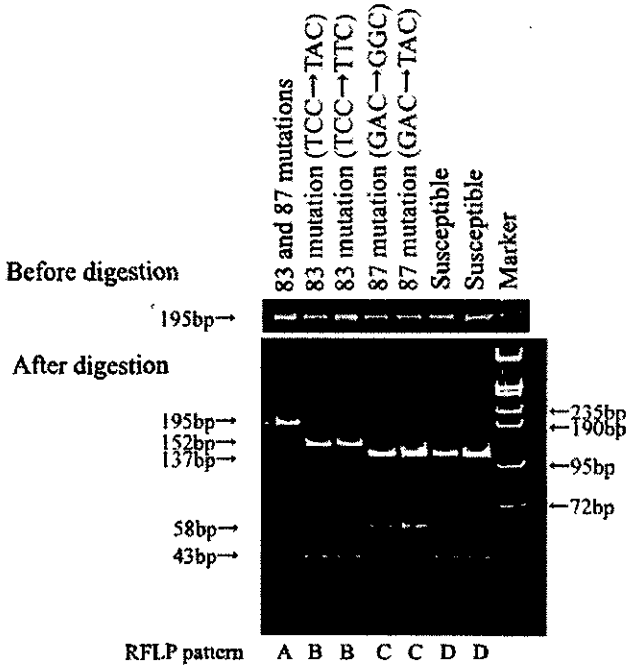

Fig. 1. PCR-RFLP patterns of the representative strains after *HinfI* digestion. The theoretical fragment sizes according to the *gyrA* sequence are mentioned in the text.

HinfI restriction enzyme due to the point mutations at the both sites, and the fragment size did not change after the digestion with *HinfI* (RFLP pattern A in Fig. 1). We examined 32 strains of *S. enterica* serovar Typhi and 23 strains of *S. enterica* serovar Paratyphi A, which include the fluoroquinolone resistant strains that were experimentally selected *in vitro*, the strains with reduced susceptibility to fluoroquinolone, and the fluoroquinolone susceptible strains, and we could successfully screen the strains with reduced susceptibility to fluoroquinolones by this method (Table 2). Establishment of surveillance system for the detection of *gyrA* mutations will be the most important to find out the fluoroquinolone resistance of *S. enterica* serovar Typhi and serovar Paratyphi A. PCR-RFLP method described here may be one of methods for the rapid detection of such mutations.

In conclusion, the surveillance for antimicrobial resistance of *S. enterica* serovar Typhi and serovar Paratyphi A should be continued. Particularly monitoring the emergence of strains with double mutations in the *gyrA* genes, that are fully resistant to fluoroquinolones, is important for the antimicrobial resistance surveillance of clinically relevant *S. enterica* serovar Typhi and serovar Paratyphi A.

This work was partially supported by a grant-in-aid for International Health Cooperation Research (12A-1) from the Ministry of Health, Labour and Welfare (to K.H.).

References

1) Brown, J.C., Shanahan, P.M., Jesudason, M.V., Thomson, C.J., and Amyes, S.G. 1996. Mutations responsible for reduced susceptibility to 4-quinolones in clinical isolates of multi-resistant *Salmonella typhi* in India. J. Antimicrob. Chemother. **37**: 891–900.
2) Chitnis, V., Chitnis, D., Verma, S., and Hemvani, N. 1999. Multidrug-resistant *Salmonella typhi* in India. Lancet **354**: 514–515.
3) Eykyn, S.J., and Williams, H. 1987. Treatment of multiresistant *Salmonella typhi* with oral ciprofloxacin. Lancet **2**: 1407–1408.
4) Giraud, E., Brisabois, A., Martel, J.L., and Chaslus-Dancla, E. 1999. Comparative studies of mutations in animal isolates and experimental *in vitro*- and *in vivo*-selected mutants of *Salmonella* spp. suggest a counter selection of highly fluoroquinolone-resistant strains in the field. Antimicrob. Agents Chemother. **43**: 2131–2137.
5) Hirose, K., Hashimoto, A., Tamura, K., Kawamura, Y., Ezaki, T., Sagara, H., and Watanabe, H. 2002. DNA sequence analysis of DNA gyrase and DNA topoisomerase IV quinolone resistance determining region of *Salmonella enterica* serovar Typhi and Paratyphi A. Antimicrob. Agents Chemother. **46**: 3249–3252.
6) Hirose, K., Tamura, K., Sagara, H., and Watanabe, H. 2001. Antibiotic susceptibilities of *Salmonella enterica* serovar Typhi and *S. enterica* serovar Paratyphi A isolated from patients in Japan. Antimicrob. Agents Chemother. **45**: 956–958.
7) Kato, J., Nishimura, Y., Imamura, R., Niki, H., Hiraga, S., and Suzuki, H. 1990. New topoisomerase essential for chromosome segregation in *E. coli*. Cell **63**: 393–404.
8) Kato, J., Suzuki, H., and Ikeda, H. 1992. Purification and characterization of DNA topoisomerase IV in *Escherichia coli*. J. Biol. Chem. **267**: 25676–25684.
9) Nakamura, S., Nakamura, M., Kojima, T., and Yoshida, H. 1989. *gyrA* and *gyrB* mutations in quinolone-resistant strains of *Escherichia coli*. Antimicrob. Agents Chemother. **33**: 254–255.
10) Panigrahi, D., Roy, P., and Sehgal, R. 1991. Ciprofloxacin for typhoid fever. Lancet **338**: 1601.
11) Parry, C., Wain, J., Chinh, N.T., Vinh, H., and Farrar, J.J. 1998. Quinolone-resistant *Salmonella typhi* in Vietnam. Lancet **351**: 1289.
12) Rowe, B., Ward, L.R., and Threlfall, E.J. 1995. Ciprofloxacin-resistant *Salmonella typhi* in the UK. Lancet **346**: 1302.
13) Rowe, B., Ward, L.R., and Threlfall, E.J. 1991. Treatment of multiresistant typhoid fever. Lancet **337**: 1422.
14) Threlfall, E.J., Skinner, J.A., and Ward, L.R. 2001. Detection of decreased *in vitro* susceptibility to ciprofloxacin in *Salmonella enterica* serotypes Typhi and Paratyphi A. J. Antimicrob. Chemother. **48**: 740–741.
15) Threlfall, E.J., and Ward, L.R. 2001. Decreased susceptibility to ciprofloxacin in *Salmonella enterica* serotype *typhi*, United Kingdom. Emerg. Infect. Dis. **7**: 448–450.
16) Threlfall, E.J., Ward, L.R., Skinner, J.A., Smith, H.R., and

Lacey, S. 1999. Ciprofloxacin-resistant *Salmonella typhi* and treatment failure. Lancet **353**: 1590–1591.
17) Wang, F., Gu, X.J., Zhang, M.F., and Tai, T.Y. 1989. Treatment of typhoid fever with ofloxacin. J. Antimicrob. Chemother. **23**: 785–788.
18) Yoshida, H., Bogaki, M., Nakamura, M., and Nakamura, S. 1990. Quinolone resistance-determining region in the DNA gyrase *gyrA* gene of *Escherichia coli*. Antimicrob. Agents Chemother. **34**: 1271–1272.
19) Yoshida, H., Bogaki, M., Nakamura, M., Yamanaka, L.M., and Nakamura, S. 1991. Quinolone resistance-determining region in the DNA gyrase *gyrB* gene of *Escherichia coli*. Antimicrob. Agents Chemother. **35**: 1647–1650.
20) Yoshida, H., Kojima, T., Yamagishi, J., and Nakamura, S. 1988. Quinolone-resistant mutations of the *gyrA* gene of *Escherichia coli*. Mol. Gen. Genet. **211**: 1–7.

Epidemiol. Infect. (2003), **130**, 533–539. © 2003 Cambridge University Press
DOI: 10.1017/S0950268803008264 Printed in the United Kingdom

Immunoglobulin G enzyme-linked immunosorbent assay using truncated nucleoproteins of Reston Ebola virus

T. IKEGAMI[1,2], M. SAIJO[1], M. NIIKURA[1], M. E. MIRANDA[3], A. B. CALAOR[3], M. HERNANDEZ[3], D. L. MANALO[3], I. KURANE[1], Y. YOSHIKAWA[2] AND S. MORIKAWA[1]*

[1] *Special Pathogens Laboratory, Department of Virology 1, National Institute of Infectious Diseases, 4-7-1 Gakuen, Musashimurayama, Tokyo 208-0011, Japan*
[2] *Department of Biomedical Science, Graduate School of Agricultural and Life Sciences, The University of Tokyo, 1-1-1 Yayoi, Bunkyo-ku, Tokyo 113-0032, Japan*
[3] *Veterinary Research Department, Research Institute for Tropical Medicine, Muntinlupa, Philippines*

(*Accepted 13 December 2002*)

SUMMARY

We developed an immunoglobulin G (IgG) enzyme-linked immunosorbent assay (ELISA), using partial recombinant nucleoproteins (rNP) of Reston Ebola virus (EBO-R) and Zaire Ebola virus (EBO-Z). We examined the reaction of 10 sera from cynomolgus macaques naturally infected with EBO-R to each of the partial rNP in the IgG ELISA. All the sera reacted to the C-terminal halves of the rNP of both EBO-R and EBO-Z. Most of the sera reacted to the RΔC (amino acid (aa) 360–739), and RΔ6 (aa 451–551) and/or RΔ8 (aa 631–739) at a higher dilution than to the corresponding truncated rNPs of EBO-Z. The results indicate that this IgG ELISA is useful for detecting EBO-R specific antibody, and may have a potential to discriminate EBO-R infection from other subtypes.

INTRODUCTION

Ebola virus, which belongs to the family *Filoviridae*, order *Mononegavirales*, is divided into four subtypes: Zaire Ebola virus (EBO-Z), Sudan Ebola virus (EBO-S), Côte d'Ivoire Ebola virus (EBO-CI), and Reston Ebola virus (EBO-R) [1]. Ebola virus has a negative-stranded RNA genome which encodes nucleoprotein (NP), P protein (VP35), matrix protein (VP40), glycoprotein (GP), second nucleoprotein (VP30), protein associated with the membrane (VP24), and RNA-dependent RNA polymerase (L) [2, 3]. EBO-Z, EBO-S, and EBO-CI emerged in equatorial Africa, and are known to cause haemorrhagic fevers in humans [4–6]. Experimental infection has also demonstrated that EBO-Z causes a similar fatal disease in guinea-pigs and non-human primates [7–9]. EBO-R emerged in a monkey export and breeding facility in the Philippines and caused fatal illness among non-human primates [10, 11]. EBO-R-infected monkeys were exported to the United States in 1989, 1990 and 1996 [12–16], and to Italy in 1992 [17]. No symptomatic infection has been recorded in humans infected with EBO-R [11, 13, 14, 17].

The epidemiological situation concerning EBO-R in the Philippines and the other Asian countries is not known. This is partly due to the lack of an EBO-R antibody-detection test kit that can be applied to epidemiological studies [18, 19]. Recently enzyme-linked immunosorbent assay (ELISA) for detecting immunoglobulin G (IgG) to EBO-Z using the recombinant NP (rNP) has been developed [20, 21]. The use of recombinant proteins has the great advantage of preparing the antigens without any specified facility, and in modification of the antigens suitable for the assay. In the present study, we prepared a panel of the truncated rNPs of EBO-R and EBO-Z and developed

* Author for correspondence.

Table 1. *Primers for the amplification of DNA encoding EBO-R NP and EBO-Z NP*

Primers for EBO-R NP	Sequences
RES-N5F	5′-GCT GGA TCC* AGA GAA CTC GAC AGC CT-3′
RES-N5R	5′-ACC GAA TTC† GGG GTC AAT TGC ACT AT-3′
RES N6F	5′-GAC GGA TCC* GAC ACT ATC ATT CCT AAT AGT GC-3′
RES-N6R	5′-TTC GAA TTC† TCG GTG CCT GTT GTA TT-3′
RES-N7F	5′-GCA GGA TCC* GAG GAA CAA GAA GGT CA-3′
RES-N7R	5′-CTT GAA TTC† ACC GAT ATC AGG GTC TT-3′
RES-N8F	5′-GCT GGA TCC* TCA CAA TTG AAT GAA GAC C-3′
RES-N8R	5′-GTG GAA TTC† TTA CTG ATG GTG CTG CAA-3′

* *Bam*HI recognition site.
† *Eco*RI recognition site.

an IgG ELISA using the rNPs. This new IgG ELISA demonstrated high specificity and sensitivity to detect EBO-R antibodies.

METHODS

Sera

Two and four rabbits were immunized four times with the histidine-tagged entire EBO-R rNP (His-EBO-R-NP) and the entire EBO-Z rNP (His-EBO-Z-NP), respectively, using Imject-Alum (Pierce, Rockford, USA). The His-EBO-R-NP and His-EBO-Z-NP were prepared and purified as described previously [21, 22]. One cynomolgus monkey was immunized four times at 2-week intervals with the His-EBO-Z-NP using Imject-Alum. The sera were collected at 7, 30 and 73 days post immunization and used in the present study.

Ten serum samples collected from cynomolgus macaques at a monkey export and breeding facility in the Philippines (Facility A) were used. This facility had experienced an EBO-R outbreak in 1996 [11]. These sera were determined to be EBO-R antibody-positive by indirect immunofluorescence assay (IFA) [22]. Three of these 10 macaques were demonstrated to have EBO-R antigens in the sera by antigen-capture ELISA [23]. Seventy-two sera were also collected from cynomolgus monkeys at another breeding facility in the Philippines (Facility B) where no EBO-R outbreak had ever occurred. These 72 sera were found to be negative for EBO-R antibodies by IFA [22].

Preparation of the glutathione S-transferase (GST)-tagged truncated Ebola NPs

The DNAs encoding the truncated NP of EBO-R were amplified by polymerase chain reaction (PCR) from the cDNA of EBO-R (DDBJ accession no. AB050936) using the primers shown in Table 1. The PCR fragments were digested with both *Bam*HI and *Eco*RI, purified and subcloned into a pGEX-2T vector (Amersham Pharmacia Biotech, Little Chalfont, UK). The sequences of the inserts were confirmed to be identical to the originals. The GST-tagged truncated NPs were expressed in *E. coli* (BL-21 strain) and purified using glutathione Sepharose 4B column chromatography, according to the manufacturer's instructions (Amersham Pharmacia Biotech). The GST-tagged truncated EBO-R rNPs included RΔC (amino acids (aa) 360–739), RΔ5 (aa 360–461), RΔ6 (aa 451–551), RΔ7 (aa 541–640) and RΔ8 (aa 631–739). The truncated EBO-Z rNPs, ZΔC (aa 361–739), ZΔ5 (aa 361–460), ZΔ6 (aa 451–552), ZΔ7 (aa 541–640) and ZΔ8 (aa 631–739), were as previously reported [21]. The GST alone was expressed and used as the negative control antigen in the IgG ELISA.

IgG ELISA using GST-tagged truncated Ebola NPs

Wells of microtitre plates (Becton Dickinson, NJ, USA) were coated with the unified amount of RΔC, RΔ5, RΔ6, RΔ7, RΔ8, ZΔC, ZΔ5, ZΔ6, ZΔ7, ZΔ8 and GST in 100 μl of PBS, and incubated overnight at 4 °C. The amounts of the antigens were determined as described below. The plates were washed three times with phosphate-buffered saline (PBS) containing 0·05% Tween 20 (PBS-T); 200 μl of PBS-T containing 0·5% bovine serum albumin (PBS-T-BSA) was added, and incubated for 1 h at 37 °C. The wild monkey sera were diluted at 1 in 100, 1 in 400, and 1 in 1600 in PBS-T-BSA, and the hyper-immune rabbits and monkey sera were twofold serially diluted from

Table 2. *Optimization of GST-Ebola rNPs* on the ELISA plate*

	RΔC	RΔ5	RΔ6	RΔ7	RΔ8	ZΔC	ZΔ5	ZΔ6	ZΔ7	ZΔ8	GST
The amount of coated antigen (ng/well)†	82	43	39	26	28	90	47	39	18	37	22
Mean OD values‡ plus 3 standard deviation of 72 sera from Ebola uninfected monkeys§	0·04	0·03	0·04	0·04	0·02	0·09	0·04	0·04	0·02	0·03	ND¶

* RΔC (aa 360–739), RΔ5 (aa 360–461), RΔ6 (aa 451–551), RΔ7 (aa 541–640), RΔ8 (aa 631–739), ZΔC (aa 361–739), ZΔ5 (aa 361–460), ZΔ6 (aa 451–552), ZΔ7 (aa 541–640), ZΔ8 (aa 631–739).

† The amount of each GST-Ebola rNP used for IgG ELISA was determined according to the antigenicity of GST-tag using an anti-GST goat polyclonal antibody at a dilution of 1 in 500.

‡ OD value for GST was subtracted from that for each GST-Ebola rNP.

§ Cynomolgus monkeys derived from a monkey breeding facility (B) in the Philippines that have not experienced any Ebola outbreaks.

¶ Not done.

1 in 100 to 1 in 6400 in PBS-T-BSA; 100 μl of each serum dilution was added to the antigen-coated wells, and incubated for 1 h at 37 °C. After washing three times with PBS-T, the wells were reacted with 100 μl of horseradish peroxidase (HRP)-conjugated goat anti-human IgG (Zymed Laboratories Inc., CA) for monkey sera, or HRP-conjugated goat anti-rabbit IgG (Zymed Laboratories Inc.) for rabbit sera, at a dilution of 1 in 1000 in PBS-T-BSA. The plates were then incubated for 1 h at 37 °C. After washing three times with PBS-T, ABTS substrate (ABTS tablet and ABTS buffer; Roche Diagnostics, Mannheim, Germany) was added to the wells. The plates were then incubated for 30 min at room temperature and optical density (OD) at 405 nm were recorded. For each sample, the adjusted OD value was calculated by subtracting the OD of GST-coated well from that of GST-fusion antigen-coated well. The mean plus three standard deviation of the adjusted OD value of 72 serum samples from Ebola virus uninfected cynomolgus monkeys to each GST-tagged, truncated Ebola rNPs was lower than 0·1 (Table 2). Therefore, the cut-off value of the IgG ELISA was determined to be 0·1. The antibody titres of serum samples were defined as the reciprocals of the highest dilution yielding a positive value.

The optimization of GST-tagged proteins on ELISA plate

The amount of coated antigens on an ELISA plate was standardized according to the antigenicity of GST-tag. Briefly, several dilutions of the GST-tagged truncated Ebola rNPs were coated on a microtitre plate (Becton Dickinson, NJ, USA.). Then, the goat anti-GST polyclonal antibody (Amersham Pharmacia Biotech) and the HRP-conjugated anti-goat IgG rabbit polyclonal antibody (Zymed Laboratories Inc.) were added as the primary and secondary antibodies at dilutions of 1 in 500 and 1 in 1000, respectively. An OD value of 0·2 was taken as the cut-off value to determine the end point dilution of each GST-tagged antigen. The dilution of eight times lower than the each end point dilution of each GST-tagged antigen was defined as the amount of antigen coating. The amount of each GST-tagged antigen used for the IgG ELISA in this study is shown in Table 2.

Indirect immunofluorescence assay (IFA)

The entire NP of EBO-R or EBO-Z was stably expressed in HeLa cells as reported previously [22, 24].

The HeLa cells were trypsinized, washed with PBS, spotted on 14-well Teflon-coated slide glasses (AR Brown Co., Ltd., Tokyo, Japan), air dried and fixed with acetone at room temperature for 5 min. The slides were stored at −80 °C until use. The slides were thawed and dried just before use; 20 μl of diluted serum was spotted on the well of the slide, and incubated under humidified conditions at 37 °C for 1 h. After washing with PBS, the slides were reacted with fluorescein isothiocyanate (FITC)-conjugated goat anti-human IgG antibody (Zymed Laboratories Inc.) at a dilution of 1 in 100 or with FITC-conjugated goat anti-rabbit IgG (Zymed Laboratories Inc.) at a dilution of 1 in 100. The slides were washed with PBS and examined for staining pattern under a fluorescent microscope. The antibody titre in the IFA was defined as the reciprocal of the highest dilution showing positive staining.

RESULTS

Reaction of hyper-immune sera to each truncated rNP of EBO-R and EBO-Z in the IgG ELISA

Reaction of EBO-R or EBO-Z hyper-immune rabbit sera and the EBO-Z hyper-immune monkey sera were examined by the IgG ELISAs with truncated EBO-R rNPs or EBO-Z rNPs (Fig. 1*a*, Fig. 1*b*, Table 3). The sera from EBO-R rNP-immunized rabbits (nos. 1 and 2) and those from EBO-Z rNP-immunized rabbits (nos. 3–6) reacted to RΔC, RΔ8, ZΔC and ZΔ8 at the titre of 6400 (Table 3). All the sera from EBO-R rNP-immunized rabbits reacted to RΔ5, RΔ6, RΔ7 and RΔ8, while the sera did not react to ZΔ6 and ZΔ7. On the other hand, all the sera from EBO-Z rNP-immunized rabbits reacted to ZΔ5, ZΔ6 and ZΔ8, while two of them did not react to RΔ6 and RΔ7.

The sera serially collected from the monkey immunized with the EBO-Z rNP were also examined (Fig. 1*b*, Table 3). The day 7 serum reacted to ZΔC, ZΔ5 and ZΔ6. The day 30 serum reacted to ZΔC, ZΔ5, ZΔ6 and ZΔ7, and the day 73 serum reacted to ZΔC, ZΔ5 and ZΔ6 at higher titres. Furthermore, the day 73 serum also reacted to ZΔ8, RΔC, RΔ5 and RΔ6.

Reaction of the sera from EBO-R infected monkeys to each truncated rNP of EBO-R and EBO-Z in the IgG ELISA

Ten IFA antibody positive monkey sera collected at the Facility A in the Philippines were examined for the reaction in the IgG ELISA (Fig. 1*c*, Table 3). All the sera reacted to RΔC and ZΔC. Seven, 9, 5 and 7 of the 10 sera reacted to RΔ5, RΔ6, RΔ7 and RΔ8,

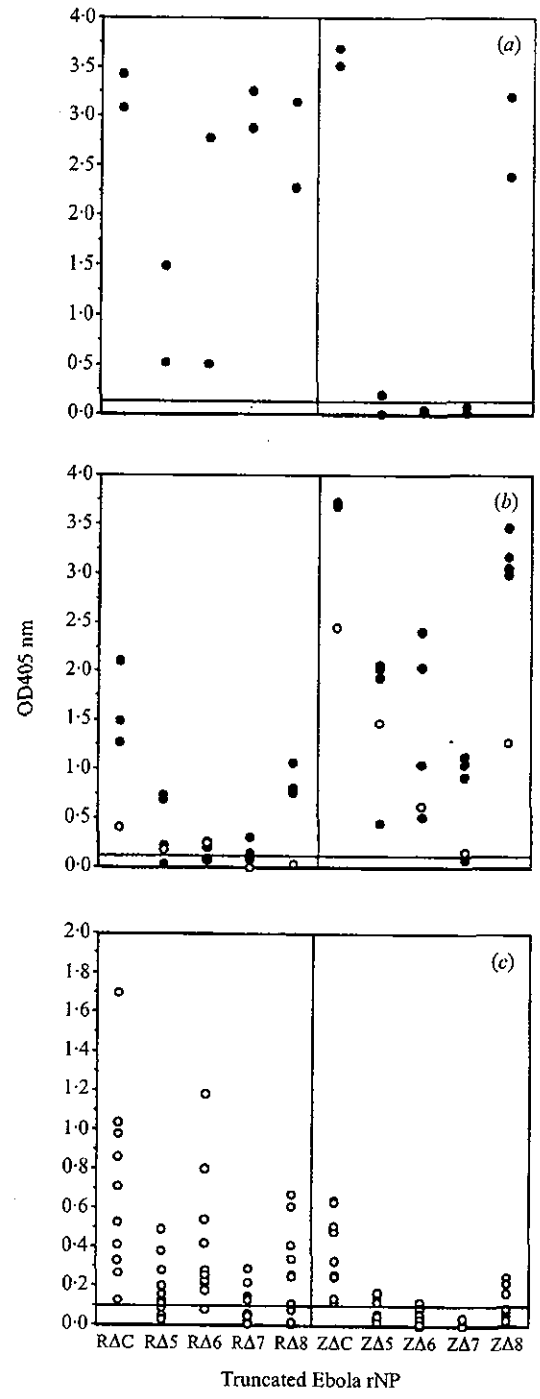

Fig. 1. The OD values at 405 nm in the IgG ELISA using truncated Ebola rNPs. (*a*) sera collected from two rabbits immunized with EBO-R rNP, (*b*) sera collected from four rabbits immunized with EBO-Z rNP (●) and from one monkey immunized with EBO-Z rNP at day 73 (○), (*c*) sera from 10 EBO-R infected monkeys. Each serum was tested at 1 in 100 dilution.

Table 3. *The reactivities of hyper-immune sera and the sera from cynomolgus monkeys naturally infected with EBO-R to the truncated rNPs* of EBO-R and EBO-Z in the IgG-ELISA*

	Titre with EBO-R rNP					Titre with EBO-Z rNP					IFA titre	
Serum samples	RΔC	RΔ5	RΔ6	RΔ7	RΔ8	ZΔC	ZΔ5	ZΔ6	ZΔ7	ZΔ8	EBO-R	EBO-Z
I. Rabbits immunized with EBO-R rNP												
No. 1	>6400†	>6400	>6400	>6400	>6400	>6400	400	—	—	>6400	2560	320
No. 2	>6400	800	400	>6400	>6400	>6400	—	—	—	>6400	1280	1280
II. Rabbits immunized with EBP-Z rNP												
No. 3	>6400	200	200	100	>6400	>6400	>6400	>6400	3200	>6400	2560	2560
No. 4	>6400	—	—	—	>6400	>6400	800	800	—	>6400	1280	5120
No. 5	>6400	1600	—	—	>6400	>6400	>6400	3200	>6400	>6400	2560	5120
No. 6	>6400	3200	200	400	>6400	>6400	>6400	>6400	>6400	>6400	40960	81920
III. A monkey immunized with EBO-Z rNP												
Day 7	—	—	—	—	—	200	100	800	—	—	<20	<20
Day 30	—	—	—	—	—	800	400	800	100	—	160	1280
Day 73	400	100	200	—	—	>6400	>6400	3200	100	3200	1280	5120
IV. EBO-R infected monkeys in Facility A‡												
No. 2728§	>1600	—	>1600	—	—	100	—	—	—	—	1280	320
No. 2669§	400	100	400	—	—	100	—	100	—	—	2560	640
No. 2921	>1600	—	400	400	—	100	—	—	—	—	1280	320
No. 2194	>1600	400	>1600	100	400	400	100	—	—	—	5120	2560
No. 2739§	100	—	—	100	100	100	—	—	—	—	1280	1280
No. 2408	>1600	100	>1600	400	>1600	400	—	—	—	100	10240	1280
No. 2190	400	100	100	—	100	100	100	—	—	—	160	160
No. 2191	400	100	100	—	400	400	100	—	—	100	640	640
No. 2195	>1600	400	>1600	100	>1600	400	—	—	—	100	2560	1280
No. 2180	>1600	400	100	—	400	400	—	—	—	100	1280	160

* RΔC (aa 360–739), RΔ5 (aa 360–461), RΔ6 (aa 451–551), RΔ7 (aa 541–640), RΔ8 (aa 631–739), ZΔC (aa 361–739), ZΔ5 (aa 361–460), ZΔ6 (aa 451–552), ZΔ7 (aa 541–640), ZΔ8 (aa 631–739).

† OD of GST-Ebola rNPs was subtracted by that of GST, and the cut off value was determined to be 0·1 on the basis of the results of 72 Ebola virus uninfected sera.

‡ Several EBO-R outbreaks have occurred in Facility A in the Philippines.

§ EBO-R NP antigens were detected from the sera of Nos. 2728, 2669 and 2739 by antigen-capture ELISA [23] at the dilution of 1 in 20, 1 in 640 and 1 in 320, respectively. The (—) means negative at a dilution of 1 in 100.

respectively. Three, 1 and 4 of the 10 sera reacted to ZΔ5, ZΔ6 and ZΔ8, respectively, while none reacted to ZΔ7. The titres were at least 4 times higher for RΔC than for ZΔC in 8 of the 10 sera in the IgG. However, only 5 sera reacted to EBO-R rNP at least 4 times higher titre than to EBO-Z rNP in IFA.

DISCUSSION

In the present study, we developed the IgG ELISAs using the truncated rNPs of Ebola viruses. The reactions of Ebola antibody positive sera to the truncated rNPs of EBO-R and EBO-Z were analysed by the IgG ELISA. The truncated rNPs used in the IgG ELISAs covered the C-terminal halves of the NPs of EBO-R and EBO-Z. It has been reported that the C-terminal halves of the NPs are hydrophilic and antigenic, while the N-terminal halves are hydrophobic and far less antigenic [19, 21, 25].

All the hyper-immune rabbit sera reacted strongly to RΔC, RΔ8, ZΔC and ZΔ8 in the IgG ELISA. The EBO-Z rNP-immune monkey serum collected on day 73 after immunization reacted to ZΔC and RΔC. Ten sera from EBO-R infected monkeys that died or were sacrificed during the EBO-R outbreak in the Philippines in 1996 were also examined by the IgG ELISA. These 10 sera were confirmed to be EBO-R antibody positive by IFA. All the 10 sera reacted to RΔC and ZΔC in the IgG ELISA. Seven of the 10 sera also reacted to RΔ8, and four (nos. 2408, 2191, 2195 and 2180) of them further cross-reacted to ZΔ8. Similar reaction pattern was demonstrated by Western blotting (data not shown). The results suggest that ΔC and Δ8 contains cross-reactive epitopes between EBO-R and EBO-Z, and that the IgG ELISA using RΔC has a suitable degree of sensitivity compared with IFA using HeLa cells expressing EBO-R rNP. Eight of the 10 sera from EBO-R infected monkeys reacted to RΔC at least 4 times higher titre than to ZΔC in the IgG ELISA, while only 5 sera reacted to EBO-R rNP at least 4 times higher titre than to EBO-Z rNP in IFA. Recent reports demonstrated that humoral immune responses were mainly directed against the NP and the VP40 in Ebola virus infected humans [26, 27]. Therefore, the IgG ELISA using RΔC and ZΔC would be useful for detecting subtype-specific antibodies. Furthermore, 6 and 5 of the 10 sera reacted to RΔ6 and RΔ8 at a dilution of 1 in 400 or greater, respectively. The results suggest that the reaction to RΔC, RΔ6 and/or RΔ8 can be considered as a clue for truly positive reaction.

Several diagnostic methods have been developed to detect Ebola-specific antibodies. It has been reported that many of these methods lack the specificity in detecting past filovirus infections. Thus, previous serological surveys could not illustrate the epidemiology of the filoviruses [18, 19]. In this regard, the newly developed IgG ELISA using the truncated rNPs might be more useful for seroepidemiological studies, especially in combination with IFA using HeLa cells expressing Ebola rNP [22, 24].

ACKNOWLEDGEMENTS

We gratefully acknowledge Ms M. Ogata of National Institute of Infectious Diseases and the staff of the Research Institute for Tropical Medicine for their technical assistance. We also thank Dr H. Cho and the staff of INA Research Co. for kindly providing us with the monkey sera. This work was partly supported by the grant from the Ministry of Health, Labour and Welfare, Japan.

REFERENCES

1. Feldmann H, Klenk HD, Sanchez A. Molecular biology and evolution of filoviruses. Arch Virol 1993; **7** (suppl): S81–100.
2. Ikegami T, Calaor AB, Miranda ME, et al. Genome structure of Ebola virus subtype Reston: differences among Ebola subtypes. Arch Virol 2001; **146**: 2021–7.
3. Sanchez A, Kiley MP, Holloway BP, Auperin DD. Sequence analysis of the Ebola virus genome: organization, genetic elements, and comparison with the genome of Marburg virus. Virus Res 1993; **29**: 215–40.
4. Le Guenno B, Formentry P, Wyers M, Gounon P, Walker F, Boesch C. Isolation and partial characterization of a new strain of Ebola virus. Lancet 1995; **345**: 1271–4.
5. World Health Organization. Ebola Haemorrhagic fever in Sudan, 1976. Bull WHO 1976; **56**: 247–70.
6. World Health Organization. Ebola haemorrhagic fever in Zaire, 1976. Report of an international commission. Bull WHO 1978; **56**: 271–93.
7. Connolly BM, Steele KE, Davis KJ, et al. Pathogenesis of experimental Ebola virus infection in guinea pigs. J Infect Dis 1999; **179** (suppl 1): S203–17.
8. Ryabchikova EI, Kolesnikova LV, Luchko SV. An analysis of features of pathogenesis in two animal models of Ebola virus infection. J Infect Dis 1999; **179**: S199–202.
9. Ryabchikova, E, Kolesnikova L, Smolina M, et al. Ebola virus infection in guinea pigs: presumable role of granulomatous inflammation in pathogenesis. Arch Virol 1996; **141**: 909–21.

10. Hayes CG, Burans JP, Ksiazek TG, et al. Outbreak of fatal illness among captive macaques in the Philippines caused by an Ebola-related filovirus. Am J Trop Med Hyg 1992; **46**: 664–71.
11. Miranda ME, Ksiazek TG, Retuya TJ, et al. Epidemiology of Ebola (subtype Reston) virus in the Philippines, 1996. J Infect Dis 1999; **179** (Suppl 1): S115–9.
12. Center for Disease Control. Ebola-Reston virus infection among quarantined nonhuman primates – Texas, 1996. MMWR 1996; **45**: 314–6.
13. Center for Disease Control. Epidemiologic notes and reports updates: filovirus infection in animal handlers. MMWR 1990; **39**: 221.
14. Center for Disease Control. Update: filovirus infections among persons with occupational exposure to nonhuman primates. MMWR 1990; **39**: 266–73.
15. Jahrling PB, Geisbert TW, Dalgard DW, et al. Preliminary report: isolation of Ebola virus from monkeys imported to USA. Lancet 1990; **335**: 502–5.
16. Rollin PE, Williams RJ, Bressler DS, et al. Ebola (subtype Reston) virus among quarantined nonhuman primates recently imported from the Philippines to United States. J Infect Dis 1999; **179** (Suppl 1): S108–14.
17. World Health Organization. Viral haemorrhagic fever in imported monkeys. Wkly Epidemiol Rec 1992; **67**: 142–3.
18. Fisher-Hoch SP, McCormick JB. Experimental filovirus infections. Curr Top Microbiol Immunol 1999; **235**: 117–43.
19. Sanchez A, Khan AS, Zaki SR, Nabel GJ, Ksiazek TG, Peters CJ. Filoviridae: Marburg and Ebola viruses. *In*: Knipe DM, Howley PM, eds. Fields Virology, 4th ed. Philadelphia, PA: Lippincott Williams & Wilkins, 2001: 1279–304.
20. Prehaud C, Hellebrand E, Coudrier D, et al. Recombinant Ebola virus nucleoprotein and glycoprotein (Gabon 94 strain) provide new tools for the detection of human infections. J Gen Virol 1998; **79**: 2565–72.
21. Saijo M, Niikura M, Morikawa S, et al. Enzyme-linked immunosorbent assays for detection of antibodies to Ebola and Marburg viruses using recombinant nucleoproteins. J Clin Microbiol 2001; **39**: 1–7.
22. Ikegami T, Saijo M, Niikura M, et al. Development of an immunofluorescence method for the detection of antibodies to Ebola virus subtype Reston by the use of recombinant nucleoprotein-expressing HeLa cells. Microbiol Immunol 2002; **46**: 633–8.
23. Niikura M, Ikegami T, Saijo M, Kurane I, Miranda ME, Morikawa S. Detection of Ebola viral antigen by enzyme-linked immunosorbent assay using a novel monoclonal antibody to nucleoprotein. J Clin Microbiol 2001; **39**: 3267–71.
24. Saijo M, Niikura M, Morikawa S, Kurane I. Immunofluorescence method for detection of Ebola virus immunogloblin G, using HeLa cells which express recombinant nucleoprotein. J Clin Microbiol 2001; **39**: 776–8.
25. Sanchez A, Kiley MP, Holloway BP, McCormick JB, Auperin DD. The nucleoprotein gene of Ebola virus: cloning, sequencing, and *in vitro* expression. Virology 1989; **170**: 81–91.
26. Baize S, Leroy EM, Georges-Courbot M-C, et al. Defective humoral responses and extensive intravascular apoptosis are associated with fatal outcome in Ebola virus-infected patients. Nat Med 1999; **5**: 423–6.
27. Leroy EM, Baize S, Volchkov VE, et al. Human asymptomatic Ebola infection and strong inflammatory response. Lancet 2000; **355**: 2210–5.